ELSEVIER

Remote Sensing of Environment 79 (2002) 344–354

Remote Sensing of Environment

www.elsevier.com/locate/rse

Forward and inverse modeling of land surface energy balance using surface temperature measurements

M.A. Friedl*

Department of Geography and Center for Remote Sensing, Boston University, 675 Commonwealth Avenue, Boston, MA 02215, USA

Received 1 October 1999; received in revised form 23 June 2000; accepted 15 July 2000

Abstract

Land surface temperature measurements have been widely used to estimate surface energy balance. However, because land surface temperature and energy balance both depend on a complex suite of factors, precise estimation of surface energy exchanges using thermal remote sensing is difficult. In recent years, a variety of methods have been developed that overcome previous limitations and show substantial promise for robust estimation of surface fluxes from remote sensing. This paper reviews recent progress in this domain and describes a two-layer energy balance model designed for use with thermal remote sensing. An important aspect of the model is that it is specifically designed to account for the complex micrometeorology and thermal properties of land surfaces possessing a range of density in vegetation. Further, the physics underlying this model are complementary to the physics of land surface thermal remote sensing. Comparisons between field measurements and modeled fluxes show good agreement, which suggests that the model describes land surface energy balance processes with good realism. More importantly, these results reinforce the conclusions of other recent studies that have demonstrated the compatibility of two-layer energy balance models with remote sensing observations and, by extension, the viability of using thermal remote sensing to model surface energy balance. © 2002 Elsevier Science Inc. All rights reserved.

1. Introduction

The properties of the Earth's land surfaces exert significant control on energy exchanges occurring at the land–atmosphere interface. These exchanges occur through processes associated with the surface radiation and energy balance, and are controlled by a complex suite of factors including the state of the overlying atmosphere, the roughness properties of the land surface, the amount and nature of vegetation cover, and the thermal properties and moisture content of the soil (Avissar & Verstraete, 1990; Brutsaert, 1982; Garratt, 1992; Stull, 1988). In recent years, a variety of large-scale field experiments have been conducted to study land surface–atmosphere interactions, primarily for the purpose of refining the representation of land surface processes within numerical weather forecast and climate models (Kustas, 1995). As a result, significant advances have been made in understanding interactions between the land surface and the atmosphere, and by extension, to land surface parameterizations within atmospheric models (Entekhabi, 1995; Sellers et al., 1997).

While significant progress has been made in the parameterization of land surface processes within soil–vegetation–atmosphere transfer (SVAT) schemes (see, for example, Betts, Ball, Beljaars, Miller, & Viterbo, 1996), remote sensing-based methods for initializing, updating, and validating land surface state variables within these models remain inadequate. In particular, virtually all of the dynamic components of land surfaces that influence and interact with the atmosphere are treated as prognostic variables within SVAT models (e.g., soil moisture and surface temperature). Therefore, a need exists for operational methods to monitor key variables such as vegetation density, soil moisture status, surface temperature, and energy fluxes at spatial and temporal scales that are commensurate with the needs of large-scale hydrologic and atmospheric circulation models. Because of the synoptic and repetitive coverage afforded by satellite platforms, remote sensing-based methods are well suited to this task.

With these issues in mind, the objectives of this paper are twofold. The first objective is to provide a concise overview of the basic theory, historical development, and current

* Tel.: +1-617-353-5745.
E-mail address: friedl@bu.edu (M.A. Friedl).

0034-4257/01/$ – see front matter © 2002 Elsevier Science Inc. All rights reserved.
PII: S0034-4257(01)00284-X

limitations to remote sensing of land surface energy balance. The second objective is to describe one approach to this problem that is based on a two-layer energy balance model, and to test this model using field data. The emphasis throughout is on the information content and utility of thermal remote sensing for modeling surface energy balance. To achieve these objectives, the paper is structured around three main sections. First, a brief overview is provided regarding the theory and history of thermal remote sensing of land surface energy balance. Section 3 describes the core elements of an energy balance model that is independent of remote sensing, but which provides a modeling framework that can be used in conjunction with remote sensing. Section 4 describes modifications to this model that allow it to be driven using land surface temperature measurements. To assess the viability of this modeling approach, model predictions are compared with observations from the HAPEX–Sahel field experiment. The paper concludes with a discussion of unresolved issues, specifically emphasizing considerations of scale.

2. Basic theory and historical limitations to thermal remote sensing of land surface energy balance

The direct but complex relationships among surface temperature, soil moisture, vegetation density, and energy balance have long been recognized by hydrologists and meteorologists (e.g., Carlson, Dodd, Benjamin, & Cooper, 1981; Carlson & Gillies, 1994; Idso, Jackson, & Reginato, 1975; Monteith, 1981; Price, 1982, 1989; Salvucci, 1997). Common to nearly all studies in this domain is the use of one-dimensional (1-D) models to describe the radiation, conduction, and turbulent transport mechanisms that influence surface temperature and energy balance. While many different strategies have been used, virtually all models of this nature are based on principles of energy conservation. The governing equation is, thus, the land surface energy balance equation, which dictates that net radiation (R_n) is balanced by the soil heat flux (G), sensible heat flux (H), and latent heat flux (λE) at the surface:

$$R_n + G + H + \lambda E = 0 \quad (1)$$

By convention, the direction of each of these terms is positive towards the surface and negative away from the surface. For most remote sensing-based energy balance studies, it is assumed that R_n is either known or may be easily computed, and that G is either known or may be parameterized in a straightforward fashion (e.g., as simple proportion of R_n). The two remaining terms, H and λE, are turbulent flux quantities and are the most difficult to estimate. Conventionally, these terms are modeled using 1-D flux-gradient expressions based on a convection analogue to Ohm's Law:

$$H = \frac{\rho C_p (T_o - T_a)}{r_a} \quad (2)$$

$$\lambda E = \frac{\rho C_p}{\gamma} \frac{(e_o - e_a)}{r_v + r_a} \quad (3)$$

where ρ is the density of air; C_p is the specific heat of air; T_o and e_o are the (aerodynamic) temperature and vapor pressure, respectively, of the surface at the effective level of heat and moisture exchange; T_a and e_a are the temperature and vapor pressure, respectively, of the overlying atmosphere; r_a and r_v are the aerodynamic and physiological resistances, respectively, to heat and moisture transport at the surface; and γ is the psychrometric constant.

Eqs. (1)–(3) form the basis of so-called one-layer energy balance models where no distinction is made between the energy balance, temperature, and vapor pressure regimes of the vegetation canopy and the soil surface. Remote sensing has been widely used with this type of framework to estimate the turbulent flux components of the surface energy balance, λE and H (see, for example, Kustas, Choudhury, et al., 1989; Kustas, Jackson, & Asrar, 1989). To do this, surface skin temperature obtained from remote sensing (T_s, the "radiometric surface temperature") is used as a surrogate for T_o in Eq. (2). Because r_v is difficult to predict, λE is frequently estimated as a residual from the energy balance equation based on estimates of H, G, and R_n. Over the past 15 years, several large-scale field experiments (including HAPEX (Andre, J.P., & Perrier, 1986; Gourturbe et al., 1997), FIFE (Sellers, Hall, Asrar, Strebel, & Murphy, 1992), MONSOON '90 (Kustas & Goodrich, 1994), and BOREAS (Sellers et al., 1995) have tested one-layer models in detail and have provided significant progress in the development of techniques to invert important land surface properties from remotely sensed data. At the same time, results from these experiments have illuminated weaknesses in remote sensing models and have pointed to key areas requiring future research (Hall, Huemmrich, Goetz, Sellers, & Nickeson, 1992; Kustas, 1995).

The most important limitation of thermal remote sensing for energy balance studies arises because T_s measurements acquired by thermal infrared (TIR) radiometers are not equivalent to T_o, the aerodynamic temperature of the surface (Brutsaert & Sugita 1996; Chehbouni, LoSeen, Njoku, & Monteny, 1995; Crago, 1998; Hall et al., 1992; Huband & Monteith, 1986; Sun & Mahrt, 1995; Vining & Blad, 1992). T_o is defined as the "effective" temperature of the surface for heat exchange, which is based on extrapolation of the vertical temperature profile in the surface layer using Monin–Obukhov similarity theory. Because the source of heat extends below the surface layer (i.e., within the canopy), the physical meaning of T_o is ambiguous and will vary depending on how the roughness length for heat exchange of the surface is prescribed (Qualls & Brutsaert, 1996; Sun, Massman, & Grantz, 1999).

Further, for regions characterized by fractional vegetation cover or row crops, T_s measurements often reflect a mixture of soil and canopy temperatures (Friedl & Davis, 1994;

Kustas et al., 1990). Therefore, depending on the view geometry of the sensor, the stability of the lower atmosphere and the temperature difference between the vegetation canopy and the soil background T_s can be substantially different from T_o (Hall et al., 1992; Sun & Mahrt, 1995; Vining & Blad, 1992). In addition, because the roughness lengths for momentum and heat exchange are not the same, corrections are often required to ensure that values for r_a, the aerodynamic resistance, are correct. If such corrections are not made, one-layer models often overestimate H and substantial site-dependent calibration is required to accurately predict fluxes.

One common solution to this problem has been to introduce an excess resistance term that accounts for the fact that the roughness lengths for heat and momentum are different (Kustas, Choudhury, et al., 1989; Kustas, Jackson, et al., 1989; Stewart et al., 1995). This excess resistance is referred to as the kB^{-1} parameter and is defined as $\log(z_{om}/z_{oh})$ (Brutsaert, 1982), where z_{om} is the roughness length for momentum of the surface and z_{oh} is the roughness length for heat. In practice, it has been widely demonstrated that values for kB^{-1} are highly variable in both space and time (Verhoef, de Bruin, & Van Den Hurk, 1997). Therefore, the utility of this approach is currently limited to situations where site-specific data are available for calibration purposes (Lhomme, Troulfeau, Monteny, Chehbouni, & Bauduin, 1997; Stewart et al., 1995; Troufleau, Lhomme, Monteny, & Vidal, 1997). Recently, Blumel (1999) and Massman (1999) have proposed models based on vegetation structure that may provide a theoretical basis for parameterizing kB^{-1}. However, these models require more extensive field validation before they can be used with confidence.

As an alternative, two-layer models have been developed that include representations for distinct temperature and energy balance regimes for the vegetation canopy and the soil surface (Choudhury, 1989; Choudhury & Monteith, 1988; Deardorff, 1978; Friedl, 1995; Kustas, 1990; Lhomme et al., 1997; Norman, Kustas, & Humes, 1995; Shuttleworth & Gurney, 1990; Shuttleworth & Wallace, 1985). While two-layer models are considerably more complex than one-layer models, recent work has shown them to be successful in overcoming some of the limitations described above. Specifically, two-layer models include resistances associated with boundary layers located at the surface of leaves within the canopy and at the soil surface. Therefore, corrections such as the kB^{-1} parameter are not required. In Section 3, the basic theory behind one such two-layer energy balance model is summarized.

3. A two-layer energy balance model: basic theory

In the sections that follow, the two-layer energy balance model described in Friedl (1995) is used. The basic theory behind this model was originally developed as a 1-D description of vegetation–atmosphere interaction (Shuttleworth, 1976). This description was subsequently modified to derive an energy combination theory describing the energy balance of land surfaces characterized by sparse vegetation (Shuttleworth & Wallace, 1985). The specific formulation used here includes a variety of refinements based on subsequent work by Choudhury (1989), Choudhury and Monteith (1988), Friedl (1995), and Shuttleworth and Gurney (1990).

3.1. Model description

Before considering the use of thermal remote sensing for estimation of H and λE, the basic form of the model is presented. It is important to note that the model presented in this section simulates land surface energy balance independent of remote sensing. The modifications required of this model for use with TIR measurements are described in Section 4. For the sake of brevity, only the core elements of the model are presented here. A more formal description is provided in Appendix A. For complete details, see Friedl (1995) and the papers cited therein.

The general form of the model used here is the same as that used by nearly all two-layer models (Baldocchi & Meyers, 1998). The net radiation of the surface (R_n) is partitioned between a canopy layer (R_v) and the soil surface (R_s), and separate energy balance equations are defined for each (Fig. 1). To do this, an equation based on Beer's law is used to estimate R_s:

$$R_s = R_n \exp(-C\mathrm{LAI}/\mu) \tag{4}$$

where C is an extinction coefficient for the vegetation canopy that ranges from ≈ 0.3 to 0.7 (Monteith & Unsworth, 1990), LAI is the leaf area index of the canopy, and μ is the cosine of the solar zenith angle. The value of C depends on the arrangement of canopy elements and is equal to 0.5 for canopies with a spherical (random) leaf angle distribution. R_v is, then, calculated as a residual:

$$R_v = R_n - R_s \tag{5}$$

Conventionally, G is estimated as a simple proportion ($\approx 40\%$) of R_s. However, recent work has shown that this relationship tends to vary as a function of time of day and date (Friedl, 1996). For this work, G is calculated as a function of R_s and μ:

$$G = K_G R_s \mu \tag{6}$$

where K_G is a constant that varies between 0.2 and 0.5 depending on the soil type and moisture conditions (Choudhury, Idso, & Reginato, 1987).

Using this approach, the heat exchanges at the soil surface and within the vegetation canopy are modeled using a set of six simultaneous equations defined by the scheme presented in Fig. 1. These equations describe distinct energy balance expressions for the soil surface and the vegetation canopy,

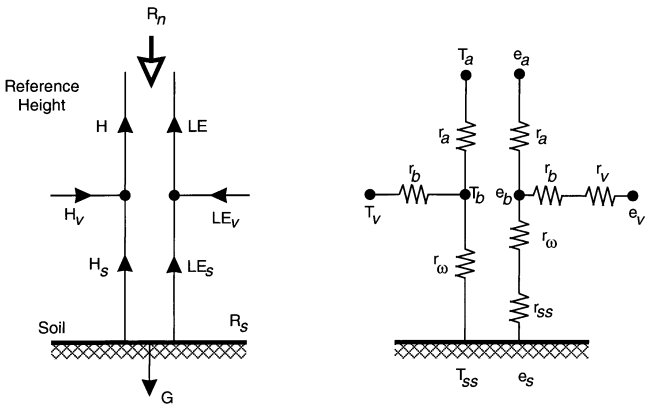

Fig. 1. Schematic describing the form of the two-layer energy balance model. The left-hand panel shows the partitioning of net radiation between the soil and canopy. The right-hand panel shows the potential–resistance network used to solve the system (from Friedl, 1995; adapted from Choudhury, 1989).

and are coupled via the aggregate energy balance of the surface. The model is driven by R_n and meteorological forcing, and requires information regarding the LAI and soil moisture conditions at the surface. Biophysical and aerodynamic resistances within the system are computed using standard methods or are prescribed (see, for example, Choudhury, 1989; Choudhury & Monteith, 1988; Shuttleworth & Gurney, 1990). The equations are then solved numerically for the unknown potentials in the system: the temperatures and vapor pressures at the soil surface (T_{ss}, e_s), at the leaf surfaces (T_v, e_v), and of the air within the canopy at the effective height of heat exchange (T_o, e_o). The fluxes of latent and sensible heat from each source (vegetation canopy and soil) and the net fluxes from the surface are then easily computed.

3.2. Simulation of energy balance and temperature regimes

The model described above can be used to simulate land surface energy balance based on forcing data and prescribed land surface conditions. In this section, this model is used to explore how variations in canopy density and surface moisture affect temperature and energy balance regimes. Thus, the key variables of interest are the canopy LAI and soil moisture, which is parameterized via the canopy stomatal resistance (r_{st}) and the soil surface resistance to evaporation (r_{ss}).

The values used for the key model inputs in the simulations that follow are presented in Tables 1 and 2. The conditions described by these simulations are representative of those encountered in the mid-latitudes at midday during the summertime. Values for forcing variables (net radiation, wind speed, air temperature, and relative humidity) were held constant while values for LAI, r_{st}, and r_{ss} were varied across realistic ranges. These two latter variables are used as surrogates for soil moisture. The values prescribed for r_{st} and r_{ss} in Table 2 are designed to simulate, in a general sense, a progression of drying that mimics the dry-down process in soils where the top layer of the soil dries first, followed by drying in the root zone. To this end, Table 2 presents the specific values and combinations used for r_{ss} and r_{st}, and indicates the relative degree of dryness versus wetness at the surface for each combination.

Table 1
Prescribed conditions used in forward mode energy balance simulations

Variable	Value/range
LAI	0–3.5
Stomatal resistance (r_{st})	200–800 s m^{-1}
Soil resistance (r_{ss})	0–2000 s m^{-1}
Net radiation (R_n)	500 W m^{-2}
Wind speed (u)	3.0 m s^{-1}
Air temperature (T_a)	300 K
Relative humidity (RH)	60%

Fig. 2 plots variation in simulated λE and H as a function of both LAI and surface moisture, and summarizes the basic control exerted by these two variables on energy partitioning at the surface. Specifically, λE varies directly with LAI, but inversely with soil moisture and vice versa for H. These patterns reflect the fact that when the overlying atmosphere is not at or near saturation, soil moisture is the dominant control on the partitioning of available energy between λE and H. As canopy density increases, λE becomes even more efficient because a larger surface area of transpiring leaves is present. Also, note that as LAI increases, R_v increases at the expense of R_s and G. Thus, while the basic relationships presented in Fig. 2 are quite straightforward, they are produced by a fairly complex and subtle set of interactions.

Fig. 3 plots modeled values for T_v and T_{ss} for the same set of conditions. As one would expect, both T_{ss} and T_v increase as r_{ss} and r_{st} increase, respectively. At the same time, both T_v and T_{ss} decrease as the canopy LAI increases. This reflects the fact that transpiring leaves provide an effective cooling mechanism for the canopy and that less energy reaches the soil surface as the canopy becomes more dense. More importantly, this figure illustrates the linkages among moisture availability, resistances to latent heat flux, and temperature regimes.

In considering these results, it is important to note that the conditions prescribed in Tables 1 and 2 are designed to illustrate the first-order relationships among temperature regimes, energy balance, soil moisture, and vegetation density. Therefore, second-order effects related to feedbacks between the surface radiation and energy balance and

Table 2
Specific values for resistances used in the simulations and their general relationship to surface moisture state

r_{ss} (s m^{-1})	r_{st} (s m^{-1})	Moisture state
0	200	Soil surface moist; root zone moist
500	200	Soil surface drying; root zone moist
1000	200	Soil surface nearly dry; root zone moist
2000	200	Soil surface completely dry; root zone moist
2000	400	Soil surface completely dry; root zone drying
2000	800	Soil surface completely dry; root zone completely dry

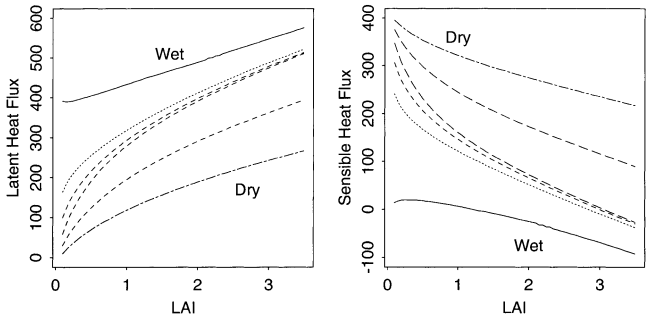

Fig. 2. Modeled latent and sensible heat fluxes (W m^{-2}) as a function of canopy density (LAI) and soil moisture availability. Forcing conditions and ranges in prescribed terms are given in Tables 1 and 2.

between surface fluxes and boundary layer properties are not included. For example, depending on wind speed, the surface skin temperature and near-surface air temperature (T_a) tend to be coupled. In a similar fashion, the vapor pressure deficit of the lower atmosphere and stomatal resistance of leaves within the canopy will covary with T_a, T_v, and T_o. Finally, because net radiation depends on the temperature of the surface, R_n should vary inversely with T_{ss} and T_v. A more realistic scenario would include covariation between these variables. However, for the objectives here (i.e., illustration), the given conditions are considered to be sufficient.

To complete this discussion, Fig. 4 plots the difference between computed values for the effective surface aerodynamic temperature (T_o) and the approximate surface radiometric temperature (T_s) that would be measured by a nadir viewing TIR instrument. To predict T_s, a geometric optical model of the upwelling thermal radiance leaving the surface was used, where T_s is a function of T_v and T_{ss}, weighted by the proportion of canopy versus soil background in the sensor field of view (Norman et al., 1995):

$$T_s = \left[f_s \times T_{ss}^4 + (1 - f_s) \times T_v^4\right]^{0.25} \quad (7)$$

where f_s is the proportion of soil background and can be easily computed from the canopy LAI (see Eq. (9)). Fig. 4 demonstrates the widely observed result that T_s tends to systematically overestimate T_o for surfaces characterized by partial canopy cover (Chehbouni et al., 1995; Lhomme, Monteny, Chehbouni, & Troufleau, 1994). Indeed, this

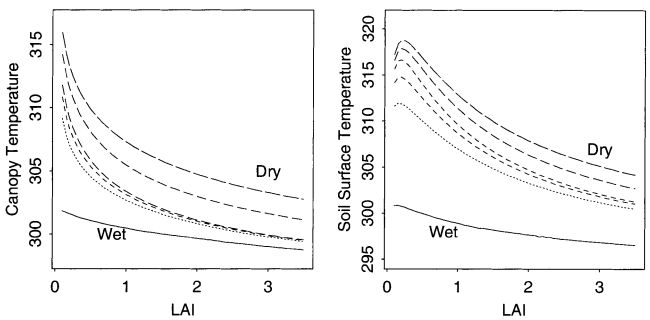

Fig. 3. Variation in modeled canopy and soil surface temperatures (K) for the conditions given in Tables 1 and 2.

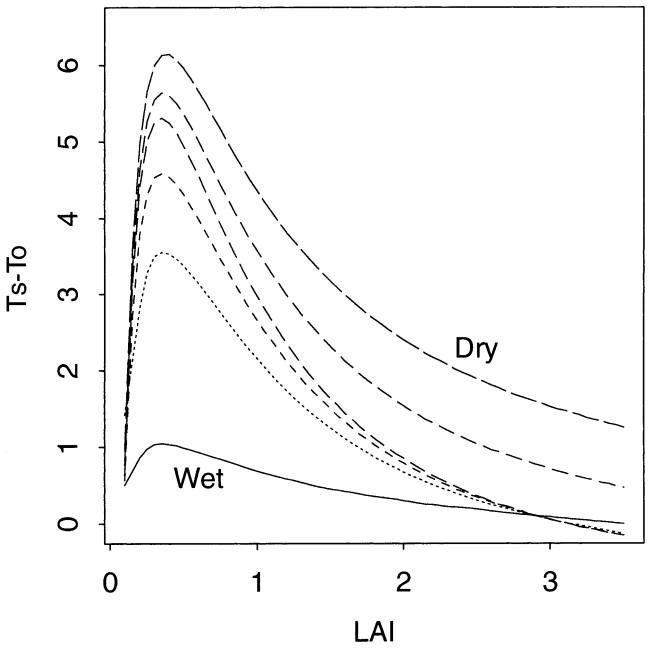

Fig. 4. Difference between modeled acrodynamic (T_o) and radiometric (T_s) temperatures (K) for the conditions prescribed in Tables 1 and 2.

difference can be dramatic for sparse canopies, even when the vegetation is only moderately stressed. More importantly, this result illustrates the main limitation of one-layer remote sensing-based energy balance models. Because T_s tends to overestimate T_o, using T_s as a surrogate for T_o can lead to substantial overestimation of H (Hall et al., 1992).

4. Modeling energy balance using surface temperature measurements

4.1. Model modifications

The two-layer model described above provides a relatively simple, yet realistic treatment of land surface energy balance. However, a key limitation of this approach is that several key variables are prescribed, most notably the soil surface and stomatal resistances to vapor transfer: r_{ss} and r_{st}, respectively. As Fig. 2 illustrates, these two variables exert strong control on the partitioning of available energy ($R_n - G$) between H and λE. In principle, these quantities may be treated as prognostic variables and predicted using a variety of different approaches (see, for example, Wallace, 1995). However, the biophysics controlling r_{ss} and r_{st} are complex and no clear consensus exists regarding how to best predict them.

At the same time, Fig. 3 demonstrates that substantial information related to moisture availability at the land surface is embedded in T_s measurements. For example, Shuttleworth and Gurney (1990) used energy combination

theory to derive expressions for canopy resistance to transpiration (r_v; the integral of r_{st} over the depth of the canopy), r_{ss}, and T_o. These expressions provide useful insights regarding the relationships among energy fluxes, moisture availability, and temperature regimes, but also require knowledge of T_{ss} and T_v, which is generally unavailable a priori.

For this work, information in T_s measurements is exploited using a somewhat different approach. The model described by Kim and Verma (1991) is used to predict r_v, and r_{ss} is treated as an additional unknown in the model. To do this, the two-layer model described in Section 3.1 is modified to use surface temperature measurements to constrain modeled values for the soil surface temperature (T_{ss}) and the vegetation canopy temperature (T_v). The upwelling thermal radiance ($L_\lambda(T_s)$) from the surface (i.e., measured by a TIR sensor) is expressed as a weighted sum of two component radiances:

$$L_\lambda(T_s) = f_s \epsilon_s L_\lambda(T_{ss}) + (1 - f_s)\epsilon_v L_\lambda(T_v) \quad (8)$$

where ϵ_v and ϵ_s are the emissivities of the vegetation and soil, L_λ is the upwelling radiance computed using the Planck equation, and T_{ss} and T_v have been previously defined. Assuming a random distribution of canopy elements, f_s is computed as a function of canopy LAI and the view geometry of the sensor:

$$f_s = \exp(-g'\mathrm{LAI}/\mu_r) \quad (9)$$

where g' is dependent on the angular distribution of canopy elements and μ_r is the cosine of the sensor view zenith angle (Choudhury, 1989).

A key attribute of this model is that it treats T_o as an unknown and solves for it numerically, rather than using a measurement of surface skin temperature (T_s) as a surrogate. This is accomplished by defining T_s according to Eq. (8) and including this expression as an additional equation in the model. In doing so, the model predicts values for T_{ss} and T_v following Eq. (8) and constrained by observations. Thus, the model is physically consistent with a geometric optical interpretation of T_s (e.g., Friedl & Davis, 1994; Kimes, 1983; Kustas et al., 1990). Further, by adding a seventh equation, the model is able to solve for r_{ss}.

4.2. Comparison of model predictions with field observations

The results that follow are based on the model described in Sections 3.1 and 4.1 using field data collected as part of the HAPEX–Sahel field experiment in 1992 in The Republic of Niger, Africa. This dataset includes measurements from multiple sites collected over several growing seasons (depending on the variable). To capture the range of variability in climate and surface conditions present within the Sahelian region, the sampling design of the experiment included three "super sites," each of which contained multiple subsites. The bulk of the measurements acquired at these super sites were collected during one intensive observation period (IOP) extending from August 15 to October 9, 1992. For further details, see Gourturbe et al. (1997).

The HAPEX–Sahel data used for this work include measurements for the month of September 1992 collected over herbaceous vegetation cover within the East Central Super Site. These data include air temperature and humidity measured at 1.8 m and wind speed measured at 10 m. Measurements of soil moisture, vegetation LAI, and canopy height were collected regularly throughout the period of interest. Surface temperature measurements were collected using an infrared radiometer with a 15° field of view placed 9 m above the surface. Estimates of in situ latent and sensible heat fluxes were computed from Bowen ratio data in association with measurements of R_n and G. All of the meteorological, energy balance, and surface temperature measurements were collected at 20-min intervals throughout the entire period of interest. For further details regarding the micrometeorological data collected as part of HAPEX–Sahel, see Gash et al. (1997). In the results presented below, only those cases where R_n was greater than 200 W m^{-2} are included.

Fig. 5 plots predicted fluxes from the model versus observed fluxes for G, λE, and H. In general, agreement between modeled and observed fluxes is good. Using $K_G = 0.23$ in Eq. (6) provides estimates of G with a root mean square error (RMSE) of 14.5 W m^{-2}, roughly within the measurement error associated with these data.

Turbulent fluxes were dominated by evaporation and the average Bowen ratio for the period of interest was only 0.62. Visual inspection of modeled versus observed fluxes for λE and H suggests that the model performs better for evaporative fluxes than for sensible heat fluxes. However, because the model is constrained to maintain energy balance for the surface, errors in H and λE are identical, but of reverse sign. Thus, the apparent superiority in model predictions for λE relative to H is a visual artifact of the smaller range in H. The overall RMSE observed in λE and H is 63.4 W m^{-2} or roughly 15% of the measured available energy ($R_n - G$). While this level of error is higher than is desirable, it is important to note that substantial uncertainty is present in the energy balance measurements.

To explore the source of model errors for H and λE, a graphical method is employed that has been previously used to examine relationships among T_a, T_o, and T_s (Chehbouni et al., 1997; Troufleau et al., 1997). This type of analysis is used here to diagnose cases identified in Fig. 5, where the two-layer model does not work well. In particular, the left-hand panel of Fig. 6 plots the relationship between $T_s - T_o$ and $T_s - T_a$, where the radius of the circle plotted for each point is proportional to the error in model predictions for each case. This plot clearly illustrates that two populations are present within the model results: one population that includes the vast majority of cases where model errors are

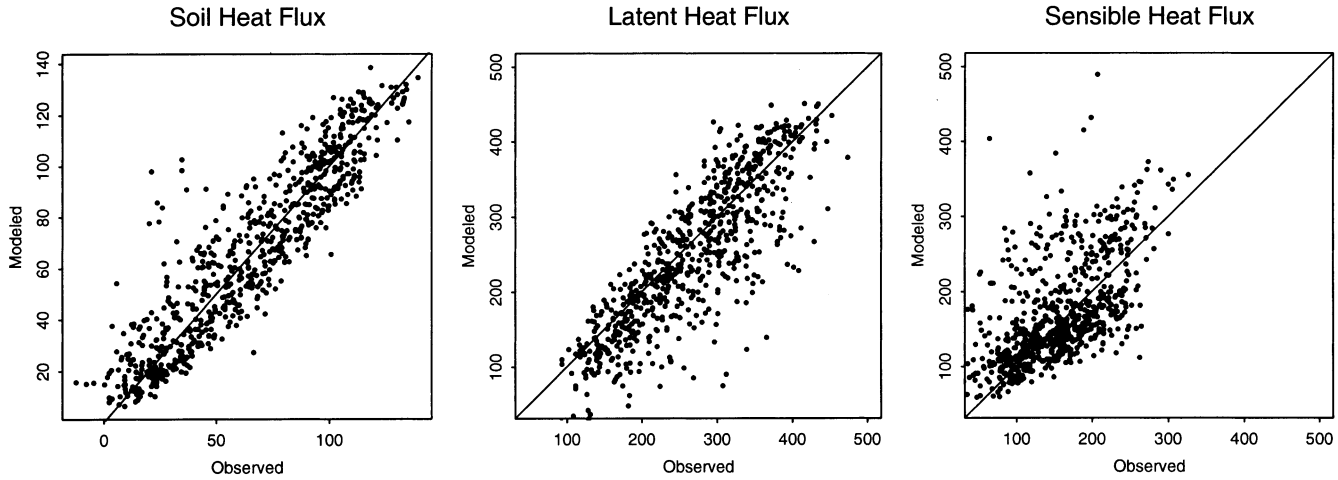

Fig. 5. Modeled versus observed energy balance components from HAPEX–Sahel. All fluxes are in units of W m^{-2}.

relatively moderate and a second smaller population for which model errors are substantially larger. Note that the cases where model errors are most pronounced tend to fall almost exactly on the one-to-one line in this plot. In other words, model errors are largest for cases where modeled T_o is equal to T_s (i.e., the equivalent of a one-layer model, excluding excess resistance terms). This result is particularly significant because the key advantage of two-layer models is that they avoid problems associated with estimation of date and time-specific excess aerodynamic resistance terms that are generally required in one-layer models. If T_o estimates derived from two-layer models are unstable or incorrect, then two-layer models provide no real advantage over one-layer models.

The right-hand panel of Fig. 6 provides insight regarding the physical mechanisms that give rise to this pattern. This figure plots T_s against wind speed, where the circles are again plotted proportional to model errors. Inspection of Fig. 6 reveals that the cases where model errors are most pronounced are associated with situations where surface temperature is high and wind speed is low. Further, these errors correspond to cases where conservation of latent heat flux is not preserved by the model (i.e., the energy balance model does not close and the estimated net flux leaving the

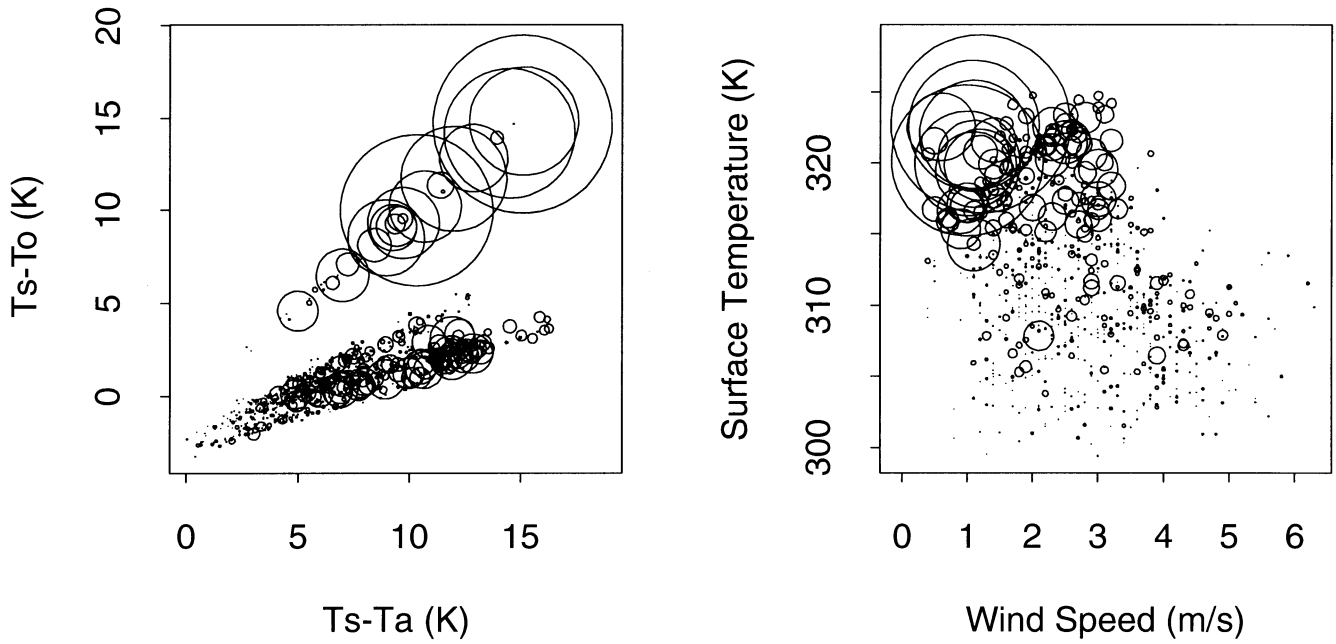

Fig. 6. $T_s - T_o$ versus $T_s - T_a$ (left) and T_s versus u (right). In both cases, the circles plotted at each point are proportional to the error in modeled fluxes. Temperatures are in units of K.

surface is not equal to the sum of the fluxes from the soil surface and the canopy). The fact that these errors are associated with cases where both H and λE are overestimated suggests that one (or more) of the aerodynamic resistance terms is underestimated for these conditions. However, further investigation is required to more precisely identify the exact nature of these errors.

5. Discussion and conclusions

This paper has reviewed methods and highlighted recent advances in coupling thermal remote sensing with land surface energy balance models. In the first part of the paper, the basic theory underlying one-layer energy balance models was discussed, emphasizing the main limitations to this type of approach. Specifically, because the radiometric skin temperature measured by remote sensing instruments is not equivalent to the surface aerodynamic temperature, one-layer models require the use of semi-empirical excess resistance terms to account for differences between the roughness lengths for heat and momentum.

In the second part of the paper, a two-layer energy balance model that is independent of remote sensing was used to demonstrate key relationships among vegetation density, soil moisture, surface temperature, and energy balance. The performance of this model coupled to TIR measurements was then tested using data from the HAPEX–Sahel field experiment. Comparison of modeled versus observed fluxes shows that the model generally predicts fluxes with good accuracy, but that both H and λE are overpredicted when wind speeds are low and T_s is high.

The two-layer model used for this work is one of several different approaches currently in active development. However, its basic elements are consistent with many current efforts in this domain. The model addresses two issues that limit the utility of one-layer models. First, the model accounts for the first-order physics (geometric optics) that strongly influence remote sensing-based measurements of surface temperature acquired from TIR instruments. Second, by computing values for the surface aerodynamic temperature in a fashion that explicitly includes treatment for boundary layer resistances at the soil and leaf surfaces, the model avoids problems associated with the use of aerodynamic resistance terms that assume identical roughness lengths for heat and momentum.

Despite this progress, a number of questions need to be resolved before remote sensing can be used to routinely estimate land surface fluxes with confidence. Perhaps the most important issue in this regard is the question of measurement and modeling scale. This issue has two distinct facets. The first facet arises from the fact that the fundamental physics that underlie all energy balance models are 1-D and assume laterally homogeneous land surface conditions. Recently, substantial effort has been devoted to developing techniques that account for spatial heterogeneity within the hydrologic and SVAT communities, and some of these approaches may be transferable to remote sensing-based models of surface energy balance (Brutsaert 1998; Giorgi & Avissar, 1997). An alternative approach, that is not discussed in this paper, is to use thermal remote sensing in association with observations or models of the planetary boundary layer to estimate regional fluxes (e.g., Brutsaert & Sugita, 1991, 1992; Carlson & Gillies, 1994; Diak, 1990; Diak & Whipple, 1993; Mecikalski, Diak, Anderson, & Norman, 1999). This issue is beginning to be addressed in the remote sensing and energy balance literature (Kustas & Norman, 1999), but further work is needed.

The second facet relates to the use of in situ measurements to validate remote sensing-based land surface energy balance models. In particular, the footprint of measurements collected from remote sensing instruments generally do not match the source area associated with surface flux measurements used for validation purposes. Such validation data are typically collected using eddy correlation or Bowen ratio energy balance instrumentation, and measured flux quantities reflect processes that have been spatially integrated by the near-surface atmosphere over the upwind fetch contributing to the flux measurements (typically hundreds of meters). Remote sensing measurements, on the other hand, possess fixed spatial resolution. As a consequence, substantial differences between modeled versus measured fluxes may arise because the remote sensing measurements reflect variability in surface properties and processes occurring at different scales from those captured in measurements of H and λE (Friedl, 1996). As remote sensing-based energy balance models move towards operational applications over large areas, continued effort will be required to address both of these questions.

Acknowledgments

This work was supported by NSF grant no. EAR-9725698 and NASA grant nos. NAG5-7217 and NAG5-8584. The efforts of HAPEX–Sahel investigators who kindly made their data available is gratefully acknowledged, especially those of D. Troufleau and J.-P. Lhomme.

Appendix A

The two-layer energy balance model used for this work is based on the general framework described in Choudhury (1989), Choudhury and Monteith (1988), and Shuttleworth and Wallace (1985), where net radiation (R_n) is partitioned between the vegetation canopy and the soil surface using an expression based on Beer's law (Eqs. (4) and (5)). The heat exchanges at each level are then modeled using a set of simultaneous equations that define coupled solutions to energy balance equations for the vegetation canopy and

Table 3
Definitions for variables within two-layer model

Variable	Definition (units)
R_s	Net radiation at soil surface (W m^{-2})
R_v	Net radiation for canopy foliage (W m^{-2})
e_s, e_v, e_o	Vapor pressure at the soil surface, foliage surface, and the effective height of heat exchange within the canopy (kPa; * indicates saturation)
T_{ss}, T_v, T_o	Temperature of the soil surface, foliage surface, and the air at effective height of heat exchange within the canopy (K)
T_a, e_a	Temperature and vapor pressure at reference height (K, kPa)
ρ	Density of air (kg m^{-3})
c_p	Specific heat of air at constant pressure (J kg^{-1} K^{-1})
γ	Psychrometric constant (kPa K^{-1})
ψ_s	Soil water potential (m)
R'	Gas constant for water vapor (m^2 s^{-2} K^{-1})
g	Acceleration due to gravity (m s^{-2})
r_b	Resistance for heat exchange between the foliage surface and the air in canopy (s m^{-1})
r_w	Resistance for heat exchange between the soil surface and the air in the canopy (s m^{-1})
r_a	Resistance for heat exchange between the air in the canopy and the air at reference height (s m^{-1})
r_v	Canopy resistance to transpiration (s m^{-1})
r_{ss}	Soil surface resistance to evaporation (s m^{-1})
ϵ_s	Emissivity of the soil surface
ϵ_v	Emissivity of the vegetation

the soil surface (definitions for the variables in each of the equations below are given in Table 3):

$$R_v = \frac{\rho C_p}{\gamma}\frac{e_v^* - e_o}{r_v + r_b} + \frac{\rho C_p}{r_b}(T_v - T_o) \quad \text{(A1)}$$

$$R_s = \frac{\rho C_p}{\gamma}\frac{e_s - e_o}{r_w + r_{ss}} + \frac{\rho C_p}{r_w}(T_{ss} - T_o) + G \quad \text{(A2)}$$

$$e_v^* = 0.611\exp\left[\frac{17.27(T_v - 273.2)}{T_v - 35.86}\right] \quad \text{(A3)}$$

$$e_s = e_s^*\exp\left[\frac{g\psi_s}{R'T_{ss}}\right] \quad \text{(A4)}$$

$$\frac{\rho C_p}{\gamma r_a}(e_o - e_a) = \frac{\rho C_p}{\gamma}\frac{(e_s - e_o)}{(r_w + r_{ss})} + \frac{\rho C_p}{\gamma}\frac{e_v^* - e_o}{r_v + r_b} \quad \text{(A5)}$$

$$\frac{\rho C_p}{r_a}(T_o - T_a) = \frac{\rho C_p}{r_w}(T_{ss} - T_o) + \frac{\rho C_p}{r_b}(T_v - T_o) \quad \text{(A6)}$$

In this set of equations, Eq. (A1) defines the energy balance of the vegetation canopy and Eq. (A2) defines the energy balance of the soil surface. Eqs. (A3) and (A4) describe the vapor pressure regimes of the canopy and soil surface, respectively, and Eqs. (A5) and (A6) require conservation of energy for the entire system for both latent and sensible heat. These six equations define a potential resistance network and are solved using the Newton–Raphson method for solution of nonlinear simultaneous equations. Given values for R_n, meteorological forcing, the canopy LAI, and the soil and canopy resistances to evaporation, this model may be used to simulate dynamics in temperature, vapor pressure, and energy balance regimes. By adding an additional equation that describes the upwelling longwave radiance from the surface as a linear combination of the radiance emitted by the vegetation canopy and soil surface weighted by the fractional coverage of vegetation (Eq. (8)), the model may be used to estimate surface energy balance as a function of surface temperature.

References

Andre, J.-C., Goutorbe, J.-P., & Perrier, A. (1986). HAPEX–MOBILHY: a hydrologic atmospheric experiment for the study of water budget and evaporation flux at the climatic scale. *Bulletin of the American Meteorological Society*, *67*, 138–144.

Avissar, R., & Verstraete, M. (1990). The representation of continental surface processes in atmospheric models. *Reviews of Geophysics*, *28*, 35–52.

Baldocchi, D., & Meyers, T. (1998). On using eco-physiological, micrometeorological and biogeochemical theory to evaluate carbon dioxide, water vapor and trace gas fluxes over vegetation: a perspective. *Agricultural and Forest Meteorology*, *90*, 1–25.

Betts, A., Ball, J., Beljaars, A., Miller, M., & Viterbo, P. (1996). The land surface–atmosphere interaction: a review based on observational and global modeling perspectives. *Journal of Geophysical Research*, *101* (D3), 7209–7225.

Blumel, K. (1999). A simple formula for estimation of the roughness length for heat transfer over partly vegetated surfaces. *Journal of Applied Meteorology*, *38*, 814–829.

Brutsaert, W. (1982). *Evaporation into the atmosphere, theory, history, and applications*. Boston, MA: Reidel.

Brutsaert, W. (1998). Land-surface water vapor and sensible heat flux: spatial variability, homogeneity, and measurement scales. *Water Resources Research*, *43*, 2433–2442.

Brutsaert, W., & Sugita, M. (1991). A bulk similarity approach in the atmospheric boundary layer using radiometric skin temperature to determine regional surface fluxes. *Boundary Layer Meteorology*, *55*, 1–23.

Brutsaert, W., & Sugita, M. (1992). Regional surface fluxes from satellite-derived surface temperatures (AVHRR) and radiosonde data. *Boundary Layer Meteorology*, *58*, 355–366.

Brutsaert, W., & Sugita, M. (1996). Sensible heat transfer parameterization for surfaces with anisothermal dense vegetation. *Journal of Atmospheric Science*, *53*, 209–216.

Carlson, T., Dodd, J., Benjamin, S., & Cooper, J. (1981). Satellite estimation of the surface energy balance, moisture availability and thermal inertia. *Journal of Applied Meteorology*, *20*, 67–87.

Carlson, T., & Gillies, R. (1994). A method to make use of thermal infrared temperature and NDVI measurements to infer surface soil water content and fractional vegetation cover. *Remote Sensing Reviews*, *9*, 161–173.

Chehbouni, A., LoSeen, D., Njoku, E., Lhomme, J.-P., Monteny, B., & Kerr, Y. (1997). Estimation of sensible heat flux over sparsely vegetated surfaces. *Journal of Hydrology*, *188–189*, 855–868.

Chehbouni, A., LoSeen, D., Njoku, E., & Monteny, B. (1995). Examination of the difference between radiative and aerodynamic surface temperature over sparsely vegetated surfaces. *Remote Sensing of Environment*, *58*, 177–186.

Choudhury, B. (1989). Estimating evaporation and carbon assimilation using infrared temperature data: vistas in modeling. In: G. Asrar (Ed.), *Theory and applications of remote sensing* (pp. 628–690). New York: Wiley.

Choudhury, B., & Monteith, J. (1988). A four-layer model for the heat budget of homogeneous land surfaces. *Quarterly Journal of the Royal Meteorological Society*, *114*, 373–398.

Choudhury, B., Idso, S., & Reginato, R. (1987). Analysis of an empirical model for soil heat flux under a growing wheat crop for estimating evaporation by an infrared-temperature based energy balance equation. *Agricultural and Forest Meteorology*, *39*, 283–297.

Crago, R. (1998). Radiometric and equivalent isothermal surface temperatures. *Water Resources Research*, *34*, 3017–3023.

Deardorff, J. (1978). Efficient prediction of ground surface temperature and moisture with inclusion of a layer of vegetation. *Journal of Geophysical Research*, *83*, 1889–1903.

Diak, G. (1990). Evaluation of heat flux, moisture flux, and aerodynamic roughness at the land surface from knowledge of the PBL height and satellite derived skin temperatures. *Agricultural and Forest Meteorology*, *52*, 181–198.

Diak, G., & Whipple, M. (1993). Improvements to models and methods for evaluating land-surface energy balance and 'effective' roughness using radiosonde reports and satellite measured 'skin' temperature data. *Agricultural and Forest Meteorology*, *63*, 189–213.

Entekhabi, D. (1995). Recent advances in land–atmosphere interaction research. *Reviews of Geophysics*, *33* (Suppl. S), 995–1003 (Part 2).

Friedl, M. (1995). Modeling land surface fluxes using a sparse canopy model and radiometric surface temperature measurements. *Journal of Geophysical Research*, *100* (D12), 25,435–25,446.

Friedl, M. (1996). Relationships among remotely sensed data, surface energy balance, and area-averaged fluxes over partially vegetated land surfaces. *Journal of Applied Meteorology*, *35* (11), 2091–2103.

Friedl, M., & Davis, F. (1994). Sources of variation in radiometric surface temperature over a tallgrass prairie. *Remote Sensing of Environment*, *48*, 1–17.

Garratt, J. (1992). *The atmospheric boundary layer*. New York, NY: Cambridge University Press.

Gash, J., Kabat, P., Monteny, B., Amadou, M., Bessemoulin, P., Billing, H., Blyth, E., De Bruin, H., Elbers, J., Friborg, T., Harrison, G., Holwill, C., Lloyd, C., Lhomme, J.-P., Moncrieff, J., Puech, D., Soegaard, H., Taupin, J., Tuzet, A., & Verhoef, A. (1997). The variability of evaporation during the HAPEX–Sahel intensive observation period. *Journal of Hydrology*, *188–189*, 385–399.

Giorgi, F., & Avissar, R. (1997). Representation of heterogeneity effects in earth system modeling: experience from land surface modeling. *Reviews of Geophysics*, *35* (4), 413–438.

Gourturbe, J., Lebel, T., Dolman, A., Gash, J., Kabat, P., Kerr, Y., Monteny, B., Prince, S., Stricker, J., Tinga, A., & Wallace, J. (1997). An overview of HAPEX–Sahel: a study in climate and desertification. *Journal of Hydrology*, *188–189*, 4–17.

Hall, F., Huemmrich, K., Goetz, S., Sellers, P., & Nickeson, J. (1992). Satellite remote sensing of surface energy balance: success failures and unresolved issues in FIFE. *Journal of Geophysical Research*, *97*, 19,061–19,089.

Huband, N., & Monteith, J. (1986). Radiative surface temperature and energy balance of a wheat canopy: I. Comparison of radiative and aerodynamic temperatures. *Boundary Layer Meteorology*, *36*, 106–116.

Idso, S., Jackson, R., & Reginato, R. (1975). Estimating evaporation: a technique adaptable to remote sensing. *Science*, *189*, 991–992.

Kim, J., & Verma, S. (1991). Modeling canopy stomatal conductance in a temperature grassland ecosystem. *Agricultural and Forest Meteorology*, *55*, 149–166.

Kimes, D. (1983). Remote sensing of row crop structure and component temperatures using directional radiometric temperatures. *Remote Sensing of Environment*, *13*, 33–55.

Kustas, W. (1990). Estimates of evapotranspiration with a one- and two-layer model of heat transfer over partial canopy cover. *Journal of Applied Meteorology*, *29*, 704–715.

Kustas, W. (1995). Recent advances associated with large scale field experiments in hydrology. *Reviews of Geophysics*, *33* (Suppl. S), 959–965 (Part 2).

Kustas, W., Choudhury, B., Inoue, Y., Pinter, P., Moran, M., Jackson, R., & Reginato, R. (1990). Ground and aircraft infrared observations over a partially-vegetated area. *International Journal of Remote Sensing*, *11*, 409–427.

Kustas, W., Choudhury, B., Reginato, M. M. R., Jackson, R., Gay, L., & Weaver, H. (1989). Determination of sensible heat flux over sparse canopy using thermal infrared data. *Agricultural and Forest Meteorology*, *44*, 197–216.

Kustas, W., & Goodrich, D. (1994). Preface. *Water Resources Research*, *30* (5), 1211–1225.

Kustas, W., Jackson, R., & Asrar, G. (1989). Estimating surface energy balance components from remotely sensed data. In: G. Asrar (Ed.), *Theory and application of optical remote sensing* (pp. 604–627). New York: Wiley.

Kustas, W., & Norman, J. (1999). Evaluation of soil and vegetation heat flux predictions using a simple two-source model with radiometric temperatures for a partial canopy cover. *Agricultural and Forest Meteorology*, *94*, 13–29.

Lhomme, J.-P., Monteny, B., Chehbouni, A., & Troufleau, D. (1994). Determination of sensible heat flux over Sahelian fallow savannah using infrared thermometry. *Agricultural and Forest Meteorology*, *68*, 93–105.

Lhomme, J.-P., Troufleau, D. D., Monteny, B., Chehbouni, A., & Bauduin, S. (1997). Sensible heat flux and radiometric surface temperature over sparse Sahelian vegetation: II. A model for the kB^{-1} parameter. *Journal of Hydrology*, *188–189*, 839–854.

Massman, W. (1999). A model study of kB_H^{-1} for vegetated surfaces using 'localized near-field' Lagrangian theory. *Journal of Hydrology*, *233*, 27–43.

Mecikalski, J., Diak, G., Anderson, M., & Norman, J. (1999). Estimating fluxes on continental scales using remotely sensed data in an atmospheric–land exchange model. *Journal of Applied Meteorology*, *38*, 1352–1369.

Monteith, J. (1981). Evaporation and surface temperature. *Quarterly Journal of the Royal Meteorological Society*, *107*, 1–27.

Monteith, J., & Unsworth, M. (1990). *Principles of Environmental Physics*. New York: Edward Arnold.

Norman, J., Kustas, W., & Humes, K. (1995). A two-source approach for estimating soil and vegetation energy fluxes from observations of directional radiometric surface temperature. *Agricultural and Forest Meteorology*, *77*, 263–293.

Price, J. (1982). On the use of satellite data to infer surface fluxes at meteorological scales. *Journal of Applied Meteorology*, *21*, 1111–1122.

Price, J. (1989). Quantitative aspects of remote sensing in the thermal infrared. In: G. Asrar (Ed.), *Theory and Applications of Optical Remote Sensing* (pp. 578–603). New York: Wiley.

Qualls, R., & Brutsaert, W. (1996). Effect of vegetation density on the parameterization of scalar roughness to estimate spatially distributed sensible heat fluxes. *Water Resources Research*, *32* (3), 645–652.

Salvucci, G. (1997). Soil moisture independent estimation of stage-two evaporation from potential evaporation and albedo or surface temperature. *Water Resources Research*, *33*, 111–122.

Sellers, P., Dickinson, R., Randall, D., Betts, A., Hall, F., Berry, J., Collatz, G., Denning, A., Mooney, H., Nobre, C., Sato, N., Field, C., & Henderson-Sellers, A. (1997). Modeling the exchanges of energy, water, and carbon between continents and the atmosphere. *Science*, *275*, 502–509.

Sellers, P., Hall, F., Asrar, G., Strebel, D., & Murphy, R. (1992). An overview of the First International Satellite Land Surface Climatology Project (ISLSCP) Field Experiment (FIFE). *Journal of Geophysical Research*, *97* (D17), 18,345–18,371.

Sellers, P., Hall, F., Margolis, H., Kelly, B., Baldocchi, D., den Hartog, G., Cihlar, J., Ryan, M.G., Goodison, B., Crill, P., Ranson, K.J., Lettenmaier, D., & Wickland, D.E. (1995). The BOREAL ecosystem–atmosphere study (BOREAS): an overview and early results from the 1994

field year. *Bulletin of the American Meteorological Society*, *76*, 1549–1577.

Shuttleworth, W. (1976). A one-dimensional theoretical description of the vegetation–atmosphere interaction. *Boundary Layer Meteorology*, *10*, 273–302.

Shuttleworth, W., & Gurney, R. (1990). The theoretical relationship between foliage temperature and canopy resistance in sparse crops. *Quarterly Journal of the Royal Meteorological Society*, *116*, 497–519.

Shuttleworth, W., & Wallace, J. (1985). Evaporation from sparse crops: an energy combination theory. *Quarterly Journal of the Royal Meteorological Society*, *111*, 1143–1162.

Stewart, J., Kustas, W., Humes, K., Nichols, W., Moran, M., & DeBruin, H. (1995). Sensible heat flux–radiometric surface temperature relationship for 8 semi-arid sites. *Journal of Applied Meteorology*, *33*, 1110–1117.

Stull, R. (1988). *An introduction to boundary layer meteorology*. Boston: Kluwer Academic Publishing.

Sun, J., & Mahrt, L. (1995). Relationship of surface heat flux to microscale temperature variations: application to BOREAS. *Boundary Layer Meteorology*, *76*, 291–301.

Sun, J., Massman, W., & Grantz, D. (1999). Aerodynamic variables in the bulk formulation of turbulent fluxes. *Boundary Layer Meteorology*, *91*, 109–125.

Troufleau, D., Lhomme, J., Monteny, B., & Vidal, A. (1997). Sensible heat flux and radiometric surface temperature over sparse Sahelian vegetation: I. An experimental analysis of the kB^{-1} parameter. *Journal of Hydrology*, *188–189*, 815–838.

Verhoef, A., De Bruin, H., & Van Den Hurk, B. (1997). Some practical notes on the parameter kB^{-1} for sparse vegetation. *Journal of Applied Meteorology*, *36*, 560–572.

Vining, R., & Blad, B. (1992). Estimation of sensible heat flux from remotely sensed canopy temperatures. *Journal of Geophysical Research*, *97* (D17), 18,951–18,954.

Wallace, J. (1995). Calculating evaporation — resistance to factors. *Agricultural and Forest Meteorology*, *73*, 353–366.